

Main Manuscript for

Optimum growth temperature declines with body size within fish species

Max Lindmark^{a,1}, Jan Ohlberger^b, Anna Gårdmark^c

^a Swedish University of Agricultural Sciences, Department of Aquatic Resources, Institute of Coastal Research, Skolgatan 6, Öregrund 742 42, Sweden

^b School of Aquatic and Fishery Sciences (SAFS), University of Washington, Box 355020, Seattle, WA 98195-5020, USA

^c Swedish University of Agricultural Sciences, Department of Aquatic Resources, Skolgatan 6, SE-742 42 Öregrund, Sweden

* Max Lindmark, Swedish University of Agricultural Sciences, Department of Aquatic Resources, Institute of Marine Research, Turistgatan 5, Lysekil 453 30, Sweden, Tel.: +46(0)104784137

Email: max.lindmark@slu.se

Author Contributions: ML conceived the study; ML, JO, AG designed research; ML performed research with input from JO and AG; ML, JO, AG wrote the paper and contributed to revisions of the manuscript.

Preprint Servers: bioRxiv: <https://www.biorxiv.org/content/10.1101/2021.01.21.427580v1>

Competing Interest Statement: No

Classification: BIOLOGICAL SCIENCES, Ecology

Keywords: body growth, metabolic rate, consumption rate, temperature-size rule, metabolic theory of ecology

This PDF file includes:

Main Text
Figures 1 to 4

28 **Abstract**

29 According to the temperature-size rule, warming of aquatic ecosystems is generally predicted to
30 increase individual growth rates but reduce asymptotic body sizes of ectotherms. However, we
31 lack a comprehensive understanding of how growth and key processes affecting it, such as
32 consumption and metabolism, depend on both temperature and body mass within species. This
33 limits our ability to inform growth models, link experimental data to observed growth patterns, and
34 advance mechanistic food web models. To examine the combined effects of body size and
35 temperature on individual growth, as well as the link between maximum consumption, metabolism
36 and body growth, we conducted a systematic review and compiled experimental data on fishes
37 from 59 studies that combined body mass and temperature treatments. By fitting hierarchical
38 models accounting for variation between species, we estimated how these three processes scale
39 jointly with temperature and body mass within species. We found that whole-organism maximum
40 consumption increases more slowly with body mass than metabolism, and is unimodal over the
41 full temperature range, which leads to the prediction that optimum growth temperatures decline
42 with body size. Using an independent dataset, we confirmed this negative relationship between
43 optimum growth temperature and size within fish species. Small individuals may therefore exhibit
44 increased growth with initial warming, whereas larger conspecifics could be the first to experience
45 negative impacts of warming on growth. These findings help advance mechanistic models of
46 individual growth and food web dynamics and improve our understanding of how climate warming
47 affects growth and size structure of aquatic ectotherms.

48 **Significance Statement**

49 Predicting organism responses to a warming climate requires understanding how physiological
50 processes such as feeding, metabolism, and growth depend on body size and temperature.
51 Common growth models predict declining optimum growth temperatures with body size if
52 energetic costs (metabolism) increase faster than gains (feeding) with body size. However, the
53 generality of these features has not been evaluated at the within-species level. By collating data
54 on fish through a systematic literature review, we find support for both declining net energy gain
55 and declining optimum growth temperatures with body size. This implies large individuals within
56 populations may be the first to suffer poor growth due to warming, with consequences for
57 fisheries yield and food web structure in warmer climates.

58 59 **Introduction**

60 Individual body growth is a fundamental process powered by metabolism, and thus depends on
61 body size and temperature (1). It affects individual fitness and life history traits, such as
62 maturation size, population growth rates (2), and ultimately energy transfer across trophic levels
63 (3, 4). Therefore, understanding how growth scales with body size and temperature is important
64 for predicting the impacts of global warming on the structure and functioning of ecosystems.

65
66 Global warming is predicted to lead to declining body sizes of organisms (5, 6). The temperature
67 size-rule ('TSR') states that warmer rearing temperatures lead to faster developmental times (and
68 larger initial size-at-age or size-at-life-stage), but smaller adult body sizes in ectotherms (7, 8).
69 This relationship is found in numerous experimental studies (7), is reflected in latitudinal gradients
70 (9), and is stronger in aquatic than terrestrial organisms (9, 10). Support for the TSR exists in
71 fishes, in particular in young fish, where reconstructed individual growth histories often reveal
72 positive correlations between growth rates and temperature in natural systems (11–14). However,
73 whether the positive effect of warming on growth is indeed limited to small individuals within a
74 species, as predicted by the temperature size-rule, is less clear. Negative correlations between
75 maximum size, asymptotic size or size-at-age of old fish and temperature have been found in
76 commercially exploited fish species (13, 15, 16). However, other studies, including large scale
77 experiments, controlled experiments and latitudinal studies or observational data on unexploited
78 species, have failed to find negative relationships between maximum size, growth of old fish or

mean size and temperature (14, 17–20) and differences between species may be related to life history traits and depend on local environmental conditions (20, 21).

While the support for TSR is mixed, and the underlying mechanisms are not well understood (8, 22, 23), theoretical growth models, such as Pütter growth models (24), including the von Bertalanffy growth model (VBGM) (25), commonly predict declines in asymptotic body mass with temperature and declines in optimum growth temperature with body mass, in line with the TSR (26–28). Yet, the physiological basis of these models has been questioned, as the commonly applied scaling parameters (mass exponents) tend to differ from empirical estimates (29, 30). Hence, despite attempting to describe growth from first principles, Pütter growth models can also be viewed as phenomenological. In more mechanistic growth models, the difference between energy gain and expenditure is partitioned between somatic growth and gonads (31–34). Energy gain is normally the amount of energy extracted from consumed food and expenditure is defined as maintenance, activity and feeding metabolism. These components of the energetics of growth are found in dynamic energy budget models (32, 35), including physiologically structured population models (PSPMs) (36), and size-spectrum models (37–39). Therefore, it is important to understand how consumption and metabolism rates scale with body mass and temperature in order to understand if and how growth of large fish within populations is limited by temperature, and to evaluate the physiological basis of growth models.

Moreover, the effect of body mass and temperature on growth dynamics should be evaluated over ontogeny at the intraspecific level (within species), which better represents the underlying process than interspecific data (among species) (30). For instance, we do not expect an interspecific relationship between optimum growth temperature and body mass, but within species it may have a large effect on growth dynamics. Despite this, intraspecific body mass and temperature scaling is often inferred from interspecific data, and we know surprisingly little about average relationship between consumption and metabolic exponents within species (30). Importantly, how physiological rates depend on mass and temperature within species can differ from the same relationships across species (40–42). Across species, rates are often assumed and found to scale as power functions of mass with exponents of $3/4$ for whole organism rates ($-1/4$ for mass-specific rates), exponentially with temperature, and with independent mass and temperature effects (e.g., in the Arrhenius fractal supply model (AFS) applied in the metabolic theory of ecology, MTE (1, 43, 44)). In contrast, within species deviations from a general $3/4$ mass exponent are common (42, 45, 46), rates are typically unimodal (41, 47–49) and the effects of mass and temperature can be interactive (40, 50–53) (but see Jerde *et al.* (42)). Alternative approaches that overcome these obstacles include fitting multiple regression models where coefficients for mass and temperature are estimated jointly (44), as well as fitting non-linear or polynomial models that can capture the de-activation of biological rates at higher temperatures (47, 48, 54). This requires intraspecific data with variation in both mass and temperature.

In this study, we analyze how maximum consumption, metabolism and growth rate of fish scale intraspecifically with mass and temperature. We performed a systematic literature review by searching the Web of Science Core Collection to compile datasets on individual-level maximum consumption, metabolism and growth rates of fish from experiments in which the effect of fish body mass is replicated across multiple temperatures within species (total $n=3672$, with data from 13, 20 and 34 species for each rate, respectively). We then fit hierarchical Bayesian models to estimate general intraspecific scaling parameters while accounting for variation between species. The estimated mass dependence and temperature sensitivity of mass-specific consumption and metabolism are used to quantify average changes in net energy gain (and hence, growth, assumed proportional to net energy gain) over temperature and body mass. Lastly, we compare our predicted changes in optimum growth temperature over body mass with an independent

experimental dataset on optimum growth temperatures across individuals of different sizes within species.

Results

We identified that within species of fish, mass-specific metabolic rates increase faster with body mass than maximum consumption rates, and neither of these rates conform to the commonly predicted $-1/4$ scaling with body mass (Fig. 1). We also quantified the unimodal relationship of consumption rate over the full temperature range (Fig. 2). Combined, these scaling relationships lead to the prediction, based on Pütter-type growth models, that optimum growth temperature declines with body size (Fig. 3) (26). The prediction of declining optimum growth temperatures with size was confirmed by our analysis of independent experimental growth rate data. We find that within species the optimum growth temperature declines with body size by 0.31°C per unit increase in the natural log of relative body mass (Fig. 4). Below we present the underlying results in more detail.

We found that the average intraspecific mass exponent for mass-specific consumption rate is smaller (-0.38 [-0.46 , -0.30]) than that for metabolic rate (-0.21 [-0.26 , -0.16]), based on the non-overlapping Bayesian 95% credible intervals (Fig. 1). It is also probable that the mass-specific scaling exponents differ from $-1/4$ (that is predicted by the MTE), because $> 99\%$ of the posterior distribution of the mass exponent of maximum consumption is below $-1/4$, and 95% of the posterior distribution of the mass exponent of metabolic rate is above $-1/4$. Activation energies of maximum consumption rate and metabolism are both similar (0.69 [0.54 , 0.85] and 0.62 [0.57 , 0.67] respectively; Fig. 1) and largely fall within the prediction from the MTE (0.6 - 0.7 eV) (1)). The global intraspecific intercept for routine and resting metabolic rate is estimated to be -1.93 [-2.11 , -1.74], and for standard metabolic rate it is -2.49 [-2.81 , -2.17] (*SI Appendix*, Fig. S7). Models where all coefficients varied by species were favored in terms of WAIC (M5 and M1, for consumption and metabolism, respectively) (*SI Appendix*, Table S4). We found statistical support for a species-varying mass and temperature interaction for metabolic rate. 98% of the posterior distribution of the global interaction coefficient μ_{β_3} is above 0 (*SI Appendix*, Fig. S5). The estimated coefficient is 0.018 [0.0008 , 0.0367] on the Arrhenius temperature scale, which corresponds to a decline in the mass scaling exponent of metabolic rate by 0.0026 $^{\circ}\text{C}^{-1}$. The selected model for maximum consumption rate did not include an interaction term (M5).

We estimated the parameters of the Sharpe-Schoolfield equation (Eq. 4) for temperature-dependence of consumption including data beyond peak temperature as: activation energy, $E_j = 0.58$ [0.45 , 0.74], rate at reference temperature, $C_{0j} = 0.70$ [0.52 , 0.89], temperature at which the rate is reduced to half (of the rate in the absence of deactivation) due to high temperatures, $T_h = 4.03$ [2.82 , 4.98], and the rate of the decline past the peak, $E_h = 2.64$ [2.17 , 3.22]. This shows that the relationship between consumption rate and temperature is unimodal and asymmetric, where the decline in consumption rate at high temperatures is steeper than the increase at low temperatures (Fig. 2).

The above results provide empirical support for the two criteria outlined in Morita et al., (26) that result in declining optimum temperatures with size, i.e. (i) smaller whole organism mass exponent for consumption than metabolism (Fig. 1) and (ii) that growth reaches an optimum over temperature. In our case, the second criterion is met because consumption reaches a peak over temperature (Fig. 2). We illustrate the consequence of these findings in Fig. 3, which shows that the optimum temperature for net energy gain is reached at a lower temperature for a smaller fish because of the difference in exponents and because net gain is unimodally related to temperature.

Assuming growth is proportional to net energy gain, this predicts that optimum growth temperature declines with body size.

Using independent data from growth trials across a range of body sizes and temperatures, we also find strong statistical support for a decline in optimum growth temperature with body mass within species, because 92% of the posterior density of the global slope estimate (μ_{β_1}) is below 0. The models with and without species-varying slopes were indistinguishable in terms of WAIC (*SI Appendix*, Table S5), and we present the results for the species-varying intercept and slope model, due to slightly better model diagnostics (*SI Appendix*, Fig. S24-27). The global relationship is given by the model: $T_{opt} = -0.074 - 0.31 \times m$, where m is the natural log of the rescaled body mass, calculated as the species-specific ratio of mass to maturation mass.

Discussion

In this study, we systematically analyzed the intraspecific scaling of consumption, metabolism and growth with body mass and temperature. We found strong evidence for declining optimum growth temperatures as individuals grow in size based on two independent approaches. First, we find differences in the intraspecific mass-scaling of consumption and metabolism, and a unimodal temperature dependence of consumption, which lead to predicted declines in optimum temperature for net energy gain (and hence growth) with size. Second, we confirm this prediction using intraspecific growth rate data of fish. Our analysis thus demonstrates the importance of understanding intraspecific scaling relationships when predicting responses of fish populations to climate warming.

That warming increases growth and development rates but reduces maximum or adult size is well known from experimental studies, also referred to as the temperature-size rule (TSR). Yet, the mechanisms underlying the TSR remain poorly understood. Pütter-type growth models, including the von Bertalanffy growth equation (VBGE), predict that the asymptotic size declines with warming if the ratio of the coefficients for energy gains and losses (H/K in Eq. 7) (27) declines with temperature. However, the assumptions underlying the VBGE were recently questioned because of the lack of empirical basis for the scaling exponents and the effects of those on the predicted effects of temperature on asymptotic size (29, 30). Specifically, the allometric exponent of energy gains (a) is assumed to be smaller than that of energetic costs (b) (Eq. 7). This is based on the assumption that anabolism scales with the same power as surfaces to volumes ($a = 2/3$) and catabolism, or maintenance metabolism, is proportional to body mass ($b = 1$) (25, 55). In contrast, maintenance costs are commonly thought to instead be proportional to standard metabolic rate, which in turn often is proportional to intake rates at the interspecific level (1, 30). This leads to $a \approx b$, resulting in unrealistic growth trajectories and temperature dependences of growth dynamics in Pütter models (29, 30). However, similar to how the existence of large fishes in tropical waters does not invalidate the hypothesis that old individuals of large-bodied fish may reach smaller sizes with warming, interspecific scaling parameters cannot reject or support these model predictions on growth within species. We show that the average intraspecific whole-organism mass scaling exponent of metabolism is larger than that of maximum consumption, i.e., the inequality $a < b$ holds at the intraspecific level. This implies that on average within species of fish, energetic costs increase faster with body mass than gains (all else equal). Importantly, when accounting for this difference in the exponents, and the unimodal thermal response of consumption, the thermal response of net energy gain is characterized by the optimum temperature being a function of body size (26). Therefore, empirically derived intraspecific parameterizations of simple growth models result in predictions in line with the TSR, in this case via declines in optimum growth temperatures over ontogeny rather than declines in asymptotic sizes.

Declines in optimum growth temperatures over ontogeny as a mechanism for TSR-like growth dynamics do not rely on the assumption that the ratio of the coefficients for energy gains and losses declines with temperature. In fact, we find that when using data from sub-peak

temperatures only, the average intraspecific predictions about the activation energy of metabolism and consumption do not differ substantially, which implies there is no clear loss or gain of energetic efficiency with warming within species. This is in contrast to other studies, e.g. Lemoine & Burkepile (56) and Rall *et al.* (57). However, it is in line with the finding that growth rates increase with temperature (e.g. 58), which is difficult to reconcile from a bioenergetics perspective if warming always reduced net energy gain. Our analysis instead suggests that the mismatch between gains and losses occurs when accounting for unimodal consumption rates over temperature. The match, or mismatch, between the temperature dependence of feeding vs. metabolic rates is a central question in ecology that extends from experiments to meta-analyses to food web models (56, 57, 59–61). Our study highlights the importance of accounting for non-linear thermal responses for two main reasons. First, the thermal response of net energy gain reaches a peak at temperatures below the peak for consumption. Secondly, as initial warming commonly leads to increased growth rates, the effect of warming on growth rates should depend on temperature rather than growth being assumed to be monotonically related to temperature.

Life-stage dependent optimum growth temperatures have previously been suggested as a component of the TSR (8). Although previous studies have found declines in optimum growth temperatures with body size in some species of fishes and other aquatic ectotherms (62–66), others have not (67, 68). Using systematically collated growth data from experiments with variation in both size and temperature treatments (13 species), we find that for an average fish, the optimum growth temperature declines as it grows in size. This finding emerges despite the small range of body sizes used in the experiments (only 10% of observations are larger than 50% of maturation size) (*SI Appendix*, Fig. S2). Individuals of such small relative size likely invest little energy in reproduction, which suggests that physiological constraints contribute to reduced growth performance of large compared to small fish, in addition to increasing investment into reproduction (69).

Translating results from experimental data to natural systems is challenging because maximal feeding rates, unlimited food supply, lack of predation, and constant temperatures do not reflect natural conditions, yet affect growth rates (67, 70, 71). In addition, total metabolic costs in the wild also include additional costs for foraging and predator avoidance. It is, however, typically found and assumed that standard metabolic rate and natural feeding levels are proportional to routine metabolic rate and maximum consumption rate, respectively, and thus exhibit the same mass-scaling relationships (32, 72). Intraspecific growth rates may not appear to be unimodally related to temperature when measured over a temperature gradient across populations within a species (20), because each population can be adapted to local climate conditions and thus display different temperature optima. However, each population likely has a thermal optimum for growth, which differs between individuals of different size. Hence, each population might have a unimodal relationship with temperature as it warms. This highlights the importance of understanding the time scale of environmental change in relation to that of immediate physiological responses, acclimation, adaptation and community reorganization for the specific prediction about climate change impacts.

In natural systems, climate warming may also result in stronger food limitation (71, 73). Hence, as optimum growth temperatures decline not only with size but also food availability (67, 74), and realized consumption rates are a fraction of the maximum consumption rate (20-70%) (Kitchell *et al.* 1977; Neuenfeldt *et al.* 2019), species may be negatively impacted by warming even when controlled experiments show they can maintain growth capacity at these temperatures. Supporting this point is the observation that warming already has negative or lack of positive effects on body growth in populations living at the edge of their physiological tolerance in terms of growth (12, 14).

Whether the largest fish of a population will be the first to experience negative effects of warming, as suggested by our finding that optimum growth temperature declines with body size, depends

on the environmental temperatures they typically experience compared to smaller conspecifics. They may for instance inhabit colder temperatures compared to small fish due to ontogenetic habitat shifts (75, 76); see also Heincke's law (77, 78). That said, there is already empirical evidence of the largest individuals in natural populations being the first to suffer from negative impacts of warming from heatwaves (79), or not being able to benefit from warming (14, 18). Hence, assuming that warming affects all individuals of a population equally is a simplification that can bias predictions of the biological impacts of climate change.

The interspecific scaling of fundamental ecological processes with body mass and temperature has been used to predict the effects of warming on body size, size structure, and population and community dynamics (26, 59, 80, 81). We argue that a contributing factor to the discrepancy between mechanistic growth models, general scaling theory, and empirical data has been the lack of data synthesis at the intraspecific level. The approach presented here can help overcome limitations of small data sets by borrowing information across species in a single modelling framework, while accounting for the intraspecific scaling of rates. Accounting for the faster increase in whole-organism metabolism than consumption with body size, the unimodal thermal response of consumption, and resulting size-dependence of optimum growth temperatures is essential for understanding what causes observed growth responses to global warming. Acknowledging these mechanisms is also important for improving predictions on the consequences of warming effects on fish growth for food web functioning, fisheries yields and global food production in warmer climates.

Materials and Methods

Data acquisition

We searched the literature for experimental studies evaluating the temperature response of individual maximum consumption rate (feeding rate at unlimited food supply, *ad libitum*), resting, routine and standard oxygen consumption rate as a proxy for metabolic rate (82) and growth rates across individuals of different sizes within species. We used three different searches on the Web of Science Core Collection (see *SI Appendix*, for details). In order to estimate how these rates depend on body size and temperature within species, we selected studies that experimentally varied both body size and temperature (at least two temperature treatments and at least two body masses). The average number of unique temperature treatments (temperature rounded to nearest °C) by species is 7.2 for growth and 4.3 for consumption and metabolism data). The criteria for both mass and temperature variation in the experiments reduces the number of potential data sets, as most experimental studies use either size or temperature treatments, not both. However, this criterion allows us to fit multiple regression models and estimate the effects of mass and temperature jointly, and to evaluate the probability of interactive mass- and temperature effects within species. Following common practice we excluded larval studies, which represents a life stage exhibiting different constraints and scaling relationships (40).

Studies were included if (i) a unique experimental temperature was recorded for each trial ($\pm 1^\circ\text{C}$), (ii) fish were provided food at *ad libitum* (consumption and growth data) or if they were unfed (resting, standard or routine metabolic rate), and (iii) fish exhibited normal behavior during the experiments. We used only one study per species and rate to ensure that all data within a given species are comparable as measurements of these rates can vary between studies due to e.g. measurement bias, differences in experimental protocols, or because different populations were studied (42, 83). In cases where we found more than one study for a given rate and species, we selected the most suitable study based on our pre-defined criteria (for details, see *SI Appendix*). We ensured that the experiments were conducted at ecologically relevant temperatures (*SI Appendix*, Figs. S1, S3). A more detailed description of the search protocol, data selection, acquisition, quality control, collation of additional information and standardizing of rates to common units can be found in *SI Appendix*.

We compiled four datasets: maximum consumption rate, metabolic rate, growth rate and the optimum growth temperature for each combination of body mass group and species. We compiled a total of 746 measurements of maximum consumption rate (of which 666 are below peak), 2699 measurements of metabolic rate and 227 measurements of growth rate (45 optimum temperatures) from published articles for each rate, from 20, 34 and 13 species, respectively, from different taxonomic groups, habitats and lifestyles (Table S1-S2). We requested original data from all corresponding authors of each article. In cases where we did not hear from the corresponding author, we extracted data from tables or figures using Web Plot Digitizer (84).

Model fitting

Model description

To each dataset, we fit hierarchical models with different combinations of species-varying coefficients, meaning they are estimated with shrinkage. This reduces the influence of outliers which could occur in species with small samples sizes (85, 86). The general form of the model is:

$$y_{ij} \sim N(\mu_{ij}, \sigma) \quad (1)$$

$$\mu_{ij} = \beta_{0j} + \sum_{p=1}^n (\beta_p \times x_{ip}) \quad (2)$$

$$\beta_{0j} \sim N(\mu_{\beta_0}, \sigma_{\beta_0}) \quad (3)$$

where y_{ij} is the i th observation for species j for rate y , β_{0j} is a species-varying intercept, x_{ip} is a predictor and β_p is its coefficient, with $p = 1, \dots, n$, where n is the number of predictors considered in the model (mass, temperature, and their interaction). Predictors are mean centered to improve interpretability (87). Species-level intercepts follow a normal distribution with hyperparameters μ_{β_0} (global intercept) and σ_{β_0} (between-species standard deviation). For most models we also allow the coefficient β_p to vary between species, such that β_p becomes β_{pj} and x_{ip} becomes x_{ijp} , where $\beta_{pj} \sim N(\mu_{\beta_p}, \sigma_{\beta_p})$. For each dataset, we evaluate multiple combinations of species-varying coefficients (from varying intercept to n varying coefficients). We used a mix of flat, weakly informative, and non-informative priors. For the temperature and mass coefficients we used the predictions from the MTE as the means of the normal prior distributions (1), but with large standard deviations (see *SI Appendix*, Table S3). Below we describe how the model in Eqns. 1-3 is applied to each data set.

Mass- and temperature dependence of consumption, metabolism and growth below peak temperatures

Peak temperatures (optimum in the case of growth) refer to the temperature at which the rate was maximized, by size group. For data below peak temperatures, we assumed that mass-specific maximum consumption rate, metabolism and growth scale allometrically (as a power function of the form $I = i_0 M^{b_0}$) with mass, and exponentially with temperature. Hence, after log-log (natural log) transformation of mass and the rate, and temperature in Arrhenius temperature ($1/kT$ in unit eV^{-1} , where k is Boltzmann's constant [$8.62 \times 10^{-5} \text{ eV K}^{-1}$]), the relationship between the rate and its predictors becomes linear. This is similar to the MTE, except that we estimate all coefficients instead of correcting rates, and allow not only the intercepts but also slopes to vary across species.

When applied to Eqns. 1-3, y_{ij} is the i th observation for species j of the natural log of the rate (consumption, metabolism or growth), and the predictors are m_{ij} (natural log of body mass), $t_{A,ij}$ (Arrhenius temperature, $1/kT$ in unit eV^{-1}), both of which were mean-centered, and their interaction. Body mass is in g, consumption rate in $\text{g g}^{-1} \text{ day}^{-1}$, metabolic rate in $\text{mg O}_2 \text{ g}^{-1} \text{ h}^{-1}$ and specific growth rate in unit \% day^{-1} . We use resting or routine metabolism (mean oxygen uptake of a resting unfed fish only showing some spontaneous activity) and standard metabolism (resting unfed and no activity, usually inferred from extrapolation or from low quantiles of routine metabolism, e.g. lowest 10% of measurements) to represent metabolic rate (88, 89). Routine and resting metabolism constitute 58% of the data used and standard metabolism constitutes 42%. We accounted for potential differences between these types of metabolic rate measurements by adding two dummy coded variables, $type_r$ and $type_s$, the former taking the value 0 for standard

and 1 for a routine or resting metabolic rate measurement, and vice versa for the latter variable. Thus, for metabolism, we replace the overall intercept β_{0j} in Eqns. 2-3 with β_{0rj} and β_{0sj} . β_{0sj} is forced to 0 for a species that has a routine or resting metabolic rate and vice versa. We assume these coefficients vary by species following normal distributions with global means $\mu_{\beta_{0r}}$ and $\mu_{\beta_{0s}}$, and standard deviations $\sigma_{\beta_{0r}}$ and $\sigma_{\beta_{0s}}$, i.e. $\beta_{0rj} \sim N(\mu_{\beta_{0r}}, \sigma_{\beta_{0r}})$ and $\beta_{0sj} \sim N(\mu_{\beta_{0s}}, \sigma_{\beta_{0s}})$.

Mass- and temperature dependence of consumption including beyond peak temperatures

Over a large temperature range, many biological rates are unimodal. We identified such tendencies in 10 out of 20 species in the consumption data set. To characterize the decline in consumption rate beyond peak temperature, we fit a mixed-effects version of the Sharpe Schoolfield equation (54) as parameterized in (90), to equations 1-2 with y_{ij} as rescaled consumption rates (C). Specifically, we model μ_{ij} in Eq. 1 with the Sharpe-Schoolfield equation:

$$\mu_{ij} = \frac{C_{0j}(T_C)e^{E_j(\frac{1}{kT_C} - \frac{1}{kT})}}{1 + e^{E_h(\frac{1}{kT_h} - \frac{1}{kT})}} \quad (4)$$

$$E_j \sim N(\mu_E, \sigma_E) \quad (5)$$

$$C_{0j} \sim N(\mu_{C_0}, \sigma_{C_0}) \quad (6)$$

where $C_{0j}(T_C)$ is the rate at a reference temperature T_C in Kelvin [K] (here set to 263.15), E_j [eV] is the activation energy, E_h [eV] characterizes the decline in the rate past the peak temperature and T_h [K] is the temperature at which the rate is reduced to half (of the rate in the absence of deactivation) due to high temperatures. We assume E_j and C_{0j} vary across species according to a normal distribution with means μ_E and μ_{C_0} , and standard deviations σ_E and σ_{C_0} (Eq. 5-6). Prior to rescaling maximum consumption (in unit g day^{-1}) by dividing $C_{i,j}$ with the mean within species \bar{C}_j , we mass-normalize it by dividing it with m^a where m is mass in g and a is the whole-organism mass-exponent calculated from the estimated mass-specific exponent with the log-linear model fitted to data below peak temperature. Temperature, T , is centered by subtracting the temperature at peak consumption estimated separately for each species using a linear model with a quadratic temperature term. The rescaling is done to control for differences between species with respect to the experimental temperatures relative to the temperature that maximizes their consumption rate such that data can be pooled.

Mass-dependence of optimum growth temperature

To evaluate how the optimum temperature ($t_{opt,ij}$, in degrees Celsius) for individual growth depends on body mass, we fit Eqns. 1-3 with y_{ij} as the mean-centered optimum growth temperature within species ($t_{opt,ij} = T_{opt,ij} - \bar{T}_{opt,j}$), to account for species being adapted to different thermal regimes. m_{ij} , the predictor variable for this model, is the natural log of the ratio between mass and mass at maturation within species: $m_{ij} = \ln(M_{ij}/M_{mat,j}) - \ln(\bar{M}_{ij}/\bar{M}_{mat,j})$. This rescaling is done because we are interested in examining relationships within species over "ontogenetic size", and because we do not expect an interspecific relationship between optimum growth temperature and body mass because species are adapted to different thermal regimes. We consider both the intercept and the effect of mass to potentially vary between species.

Parameter estimation

We fit the models in a Bayesian framework, using R version 4.0.2 (91) and JAGS (92) through the R-package 'rjags' (93). We used 3 Markov chains with 5000 iterations for adaptation, followed by 15000 iterations burn-in and 15000 iterations sampling where every 5th iteration saved. Model convergence was assessed by visually inspecting trace plots and potential scale reduction factors (\hat{R}) (SI Appendix). \hat{R} compares chain variance with the pooled variance, and values <1.1 suggest all three chains converged to a common distribution (94). We relied heavily on the R packages within 'tidyverse' (95) for data processing, as well as 'ggmcmc' (96), 'mcmcviz' (97) and 'bayesplot' (98) for visualization.

Model comparison

We compared the parsimony of models with different hierarchical structures, and with or without mass-temperature interactions, using the Watanabe-Akaike information criterion (WAIC) (99, 100), which is based on the posterior predictive distribution. We report WAIC for each model described above (Table S4-S5), and examine models with ΔWAIC values < 2 , where ΔWAIC is each model's difference to the lowest WAIC across models, in line with other studies (101).

Net energy gain

The effect of temperature and mass dependence of maximum consumption and metabolism (proportional to biomass gain and losses, respectively) (31, 32, 34) on growth is illustrated by visualizing the net energy gain. The model for the net energy gain (growth) can be viewed as a Pütter-type model, which is the result of two antagonistic allometric processes, biomass gains and biomass losses:

$$\frac{dM}{dt} = H(T)M^a - K(T)M^b \quad (7)$$

where M is body mass and T is temperature, H and K the allometric constants and a and b the exponents of the processes underlying gains and losses, respectively. We convert metabolism from oxygen consumption [$\text{mg O}_2 \text{ h}^{-1} \text{ day}^{-1}$] to g day^{-1} by assuming $1 \text{ kcal} = 295 \text{ mg O}_2$ (based on an oxycaloric coefficient of 14.2 J/mg O_2) (102), $1 \text{ kcal} = 4184 \text{ J}$ and an energy content of 5600 J/g (103), and convert consumption to g day^{-1} from $\text{g g}^{-1} \text{ day}^{-1}$. Consumption and metabolic rate are calculated for two sizes (5 and 1000 g, which roughly correspond to the 25th percentile of both datasets and the maximum mass in the consumption data, respectively), using the global allometric relationships found in the log-log models fit to sub-peak temperatures. These allometric functions are further scaled with the temperature correction factors r_c for consumption and r_m for metabolism. r_c is based on the Sharpe-Schoolfield model and r_m is given by the temperature dependence of metabolic rate from the log-linear model. Because r_c and r_m are fitted to data on different scales, we divide these functions by their maximum. Lastly, we rescale the product between the allometric functions and r_c and r_m such that the rate at 19°C (mean temperature in both data sets) equals the temperature-independent rate.

Acknowledgments

We thank Hiroki Yamanaka, Dennis Tomalá Solano, Vanessa Messmer, Björn Björnsson, Albert Imsland, Tomas Árnasson, Yiping Luo, Takeshi Tomiyama and Myron Peck for generously providing data; Magnus Huss and Ken Haste Andersen, for providing useful comments on earlier versions of the manuscript; Daniel Padfield and Wilco Verberk for helpful discussions; Matthew Low and Malin Aronson for an introduction to Bayesian inference. This study was supported by grants from the Swedish Research Council FORMAS (no. 217-2013-1315) and the Swedish Research Council (no. 2015-03752) (both to AG).

Data accessibility statement

All data and R code (lists of studies in literature search, data preparation, analyses and figures) can be downloaded from a GitHub repository (<https://github.com/maxlindmark/scaling>) and will be archived on Zenodo upon publication.

References

1. J. H. Brown, J. F. Gillooly, A. P. Allen, V. M. Savage, G. B. West, Toward a metabolic theory of ecology. *Ecology* **85**, 1771–1789 (2004).
2. V. M. Savage, J. F. Gillooly, J. H. Brown, G. B. West, E. L. Charnov, Effects of body size and temperature on population growth. *The American Naturalist* **163**, 429–441 (2004).

- 494 3. K. H. Andersen, J. E. Beyer, P. Lundberg, Trophic and individual efficiencies of size-
495 structured communities. *Proceedings of the Royal Society B: Biological Sciences* **276**,
496 109–114 (2009).
- 497 4. D. R. Barneche, A. P. Allen, The energetics of fish growth and how it constrains food-web
498 trophic structure. *Ecology Letters* **21**, 836–844 (2018).
- 499 5. M. Daufresne, K. Lengfellner, U. Sommer, Global warming benefits the small in aquatic
500 ecosystems. *Proceedings of the National Academy of Sciences, USA* **106**, 12788–12793
501 (2009).
- 502 6. J. L. Gardner, A. Peters, M. R. Kearney, L. Joseph, R. Heinsohn, Declining body size: a
503 third universal response to warming? *Trends in Ecology & Evolution* **26**, 285–291 (2011).
- 504 7. D. Atkinson, “Temperature and organism size—A biological law for ectotherms?” in
505 *Advances in Ecological Research*, (Elsevier, 1994), pp. 1–58.
- 506 8. J. Ohlberger, Climate warming and ectotherm body size – from individual physiology to
507 community ecology. *Functional Ecology* **27**, 991–1001 (2013).
- 508 9. C. R. Horne, Andrew. G. Hirst, D. Atkinson, Temperature-size responses match latitudinal-
509 size clines in arthropods, revealing critical differences between aquatic and terrestrial
510 species. *Ecology Letters* **18**, 327–335 (2015).
- 511 10. J. Forster, A. G. Hirst, D. Atkinson, Warming-induced reductions in body size are greater
512 in aquatic than terrestrial species. *PNAS* **109**, 19310–19314 (2012).
- 513 11. R. E. Thresher, J. A. Koslow, A. K. Morison, D. C. Smith, Depth-mediated reversal of the
514 effects of climate change on long-term growth rates of exploited marine fish. *Proceedings*
515 *of the National Academy of Sciences, USA* **104**, 7461–7465 (2007).
- 516 12. A. B. Neuheimer, R. E. Thresher, J. M. Lyle, J. M. Semmens, Tolerance limit for fish
517 growth exceeded by warming waters. *Nature Climate Change* **1**, 110–113 (2011).
- 518 13. A. R. Baudron, C. L. Needle, A. D. Rijnsdorp, C. T. Marshall, Warming temperatures and
519 smaller body sizes: synchronous changes in growth of North Sea fishes. *Global Change*
520 *Biology* **20**, 1023–1031 (2014).
- 521 14. M. Huss, M. Lindmark, P. Jacobson, R. M. Van Dorst, A. Gårdmark, Experimental
522 evidence of gradual size-dependent shifts in body size and growth of fish in response to
523 warming. *Glob Change Biol* **25**, 2285–2295 (2019).
- 524 15. I. E. Ikpewe, A. R. Baudron, A. Ponchon, P. G. Fernandes, Bigger juveniles and smaller
525 adults: Changes in fish size correlate with warming seas. *Journal of Applied Ecology* **Early**
526 **View** (2020).
- 527 16. I. van Rijn, Y. Buba, J. DeLong, M. Kiflawi, J. Belmaker, Large but uneven reduction in fish
528 size across species in relation to changing sea temperatures. *Global Change Biology* **23**,
529 3667–3674 (2017).
- 530 17. D. R. Barneche, M. Jahn, F. Seebacher, Warming increases the cost of growth in a model
531 vertebrate. *Functional Ecology* **33**, 1256–1266 (2019).
- 532 18. R. M. Van Dorst, *et al.*, Warmer and browner waters decrease fish biomass production.
533 *Global Change Biology* **25**, 1395–1408 (2019).
- 534 19. A. Audzijonyte, *et al.*, Fish body sizes change with temperature but not all species shrink
535 with warming. *Nat Ecol Evol* **4**, 809–814 (2020).
- 536 20. D. van Denderen, H. Gislason, J. van den Heuvel, K. H. Andersen, Global analysis of fish
537 growth rates shows weaker responses to temperature than metabolic predictions. *Global*
538 *Ecology and Biogeography* **29**, 2203–2213 (2020).
- 539 21. H.-Y. Wang, S.-F. Shen, Y.-S. Chen, Y.-K. Kiang, M. Heino, Life histories determine
540 divergent population trends for fishes under climate warming. *Nature Communications* **11**,
541 4088 (2020).
- 542 22. A. Audzijonyte, *et al.*, Is oxygen limitation in warming waters a valid mechanism to explain
543 decreased body sizes in aquatic ectotherms? *Global Ecology and Biogeography* **28**, 64–
544 77 (2019).
- 545 23. P. Neubauer, K. H. Andersen, Thermal performance of fish is explained by an interplay
546 between physiology, behaviour and ecology. *Conserv Physiol* **7** (2019).

- 547 24. A. Pütter, Studien über physiologische Ähnlichkeit VI. Wachstumsähnlichkeiten. *Pflügers*
548 *Arch.* **180**, 298–340 (1920).
- 549 25. L. von Bertalanffy, Laws in metabolism and growth. *The quarterly review of biology* **32**,
550 217–231 (1957).
- 551 26. K. Morita, M. Fukuwaka, N. Tanimata, O. Yamamura, Size-dependent thermal preferences
552 in a pelagic fish. *Oikos* **119**, 1265–1272 (2010).
- 553 27. D. Pauly, W. W. L. Cheung, Sound physiological knowledge and principles in modeling
554 shrinking of fishes under climate change. *Global Change Biology* **24**, e15–e26 (2018).
- 555 28. D. Pauly, The gill-oxygen limitation theory (GOLT) and its critics. *Science Advances* **7**,
556 eabc6050 (2021).
- 557 29. S. Lefevre, D. J. McKenzie, G. E. Nilsson, In modelling effects of global warming, invalid
558 assumptions lead to unrealistic projections. *Global Change Biology* **24**, 553–556 (2018).
- 559 30. D. J. Marshall, C. R. White, Have we outgrown the existing models of growth? *Trends in*
560 *Ecology & Evolution* **34**, 102–111 (2019).
- 561 31. E. Ursin, A Mathematical Model of Some Aspects of Fish Growth, Respiration, and
562 Mortality. *Journal of the Fisheries Research Board of Canada* **24**, 2355–2453 (1967).
- 563 32. J. F. Kitchell, D. J. Stewart, D. Weininger, Applications of a bioenergetics model to yellow
564 perch (*Perca flavescens*) and walleye (*Stizostedion vitreum vitreum*). *Journal of the*
565 *Fisheries Board of Canada* **34**, 1922–1935 (1977).
- 566 33. M. Jobling, “Temperature and growth: modulation of growth rate via temperature change”
567 in *Global Warming: Implications for Freshwater and Marine Fish*, C. M. Wood, D. G.
568 McDonald, Eds. (Cambridge University Press, 1997), pp. 225–254.
- 569 34. T. E. Essington, J. F. Kitchell, C. J. Walters, The von Bertalanffy growth function,
570 bioenergetics, and the consumption rates of fish. *Canadian Journal of Fisheries and*
571 *Aquatic Sciences* **58**, 2129–2138 (2001).
- 572 35. S. A. L. M. Kooijman, *Dynamic energy budgets in biological systems* (Cambridge
573 University Press, 1993).
- 574 36. A. M. de Roos, L. Persson, Physiologically structured models – from versatile technique to
575 ecological theory. *Oikos* **94**, 51–71 (2001).
- 576 37. M. Hartvig, K. H. Andersen, J. E. Beyer, Food web framework for size-structured
577 populations. *Journal of Theoretical Biology* **272**, 113–122 (2011).
- 578 38. O. Maury, J.-C. Poggiale, From individuals to populations to communities: A dynamic
579 energy budget model of marine ecosystem size-spectrum including life history diversity.
580 *Journal of Theoretical Biology* **324**, 52–71 (2013).
- 581 39. J. L. Blanchard, R. F. Heneghan, J. D. Everett, R. Trebilco, A. J. Richardson, From
582 bacteria to whales: Using functional size spectra to model marine ecosystems. *Trends in*
583 *Ecology & Evolution* **32**, 174–186 (2017).
- 584 40. D. S. Glazier, Beyond the “3/4-power law”: variation in the intra- and interspecific scaling of
585 metabolic rate in animals. *Biological Reviews of the Cambridge Philosophical Society* **80**,
586 611–662 (2005).
- 587 41. B. C. Rall, *et al.*, Universal temperature and body-mass scaling of feeding rates.
588 *Philosophical Transactions of the Royal Society of London, Series B: Biological Sciences*
589 **367**, 2923–2934 (2012).
- 590 42. C. L. Jerde, *et al.*, Strong Evidence for an Intraspecific Metabolic Scaling Coefficient Near
591 0.89 in Fish. *Front. Physiol.* **10**, 1166 (2019).
- 592 43. J. F. Gillooly, J. H. Brown, G. B. West, V. M. Savage, E. L. Charnov, Effects of size and
593 temperature on metabolic rate. *Science*, 2248–2251. (2001).
- 594 44. C. J. Downs, J. P. Hayes, C. R. Tracy, Scaling metabolic rate with body mass and inverse
595 body temperature: A test of the Arrhenius fractal supply model. *Functional Ecology* **22**,
596 239–244 (2008).
- 597 45. A. Clarke, N. M. Johnston, Scaling of metabolic rate with body mass and temperature in
598 teleost fish. *Journal of Animal Ecology* **68**, 893–905 (1999).
- 599 46. F. Bokma, Evidence against universal metabolic allometry. *Functional Ecology* **18**, 184–
600 187 (2004).

47. A. I. Dell, S. Pawar, V. M. Savage, Systematic variation in the temperature dependence of physiological and ecological traits. *Proceedings of the National Academy of Sciences* **108**, 10591–10596 (2011).
48. G. Englund, G. Öhlund, C. L. Hein, S. Diehl, Temperature dependence of the functional response. *Ecology Letters* **14**, 914–921 (2011).
49. S. F. Uiterwaal, J. P. DeLong, Functional responses are maximized at intermediate temperatures. *Ecology* **101**, e02975 (2020).
50. Xiaojun. Xie, Ruyung. Sun, The Bioenergetics of the Southern Catfish (*Silurus meridionalis* Chen). I. Resting Metabolic Rate as a Function of Body Weight and Temperature. *Physiological Zoology* **63**, 1181–1195 (1990).
51. B. García García, J. Cerezo Valverde, F. Aguado-Giménez, J. García García, M. D. Hernández, Effect of the interaction between body weight and temperature on growth and maximum daily food intake in sharpsnout sea bream (*Diplodus puntazzo*). *Aquaculture International* **19**, 131–141 (2011).
52. J. Ohlberger, Thomas. Mehner, Georg. Staaks, Franz. Hölker, Intraspecific temperature dependence of the scaling of metabolic rate with body mass in fishes and its ecological implications. *Oikos* **121**, 245–251 (2012).
53. M. Lindmark, M. Huss, J. Ohlberger, A. Gårdmark, Temperature-dependent body size effects determine population responses to climate warming. *Ecology Letters* **21**, 181–189 (2018).
54. R. M. Schoolfield, P. J. H. Sharpe, C. E. Magnuson, Non-linear regression of biological temperature-dependent rate models based on absolute reaction-rate theory. *Journal of Theoretical Biology* **88**, 719–731 (1981).
55. D. Pauly, W. W. L. Cheung, On confusing cause and effect in the oxygen limitation of fish. *Global Change Biology* **24**, e743–e744 (2018).
56. N. P. Lemoine, D. E. Burkepile, Temperature-induced mismatches between consumption and metabolism reduce consumer fitness. *Ecology* **93**, 2483–2489 (2012).
57. B. C. Rall, O. Vucic-Pestic, R. B. Ehnes, M. Emmerson, U. Brose, Temperature, predator–prey interaction strength and population stability. *Global Change Biology* **16**, 2145–2157 (2010).
58. M. J. Angilletta, A. E. Dunham, The temperature-size rule in ectotherms: simple evolutionary explanations may not be general. *The American Naturalist* **162**, 332–342 (2003).
59. D. A. Vasseur, K. S. McCann, A mechanistic approach for modelling temperature-dependent consumer-resource dynamics. *The American Naturalist* **166**, 184–198 (2005).
60. K. E. Fussmann, F. Schwarzmüller, U. Brose, A. Jousset, B. C. Rall, Ecological stability in response to warming. *Nature Climate Change* **4**, 206–210 (2014).
61. M. Lindmark, J. Ohlberger, M. Huss, A. Gårdmark, Size-based ecological interactions drive food web responses to climate warming. *Ecology Letters* **22**, 778–786 (2019).
62. J. Wyban, W. A. Walsh, D. M. Godin, Temperature effects on growth, feeding rate and feed conversion of the Pacific white shrimp (*Penaeus vannamei*). *Aquaculture* **138**, 267–279 (1995).
63. V. E. Panov, D. J. McQueen, Effects of temperature on individual growth rate and body size of a freshwater amphipod. **76**, 1107–1116 (1998).
64. A. Steinarsson, A. K. Imsland, Size dependent variation in optimum growth temperature of red abalone (*Haliotis rufescens*). *Aquaculture* **224**, 353–362 (2003).
65. B. Björnsson, A. Steinarsson, T. Árnason, Growth model for Atlantic cod (*Gadus morhua*): Effects of temperature and body weight on growth rate. *Aquaculture* **271**, 216–226 (2007).
66. S. O. Handeland, A. K. Imsland, S. O. Stefansson, The effect of temperature and fish size on growth, feed intake, food conversion efficiency and stomach evacuation rate of Atlantic salmon post-smolts. *Aquaculture* **283**, 36–42 (2008).
67. J. R. Brett, J. E. Shelbourn, C. T. Shoop, Growth rate and body composition of fingerling sockeye salmon, *Oncorhynchus nerka*, in relation to temperature and ration size. *J. Fish. Res. Bd. Can.* **26**, 2363–2394 (1969).

- 655 68. J. M. Elliott, M. A. Hurley, The functional relationship between body size and growth rate in
656 fish. *Functional Ecology* **9**, 625 (1995).
- 657 69. D. R. Barneche, D. R. Robertson, C. R. White, D. J. Marshall, Fish reproductive-energy
658 output increases disproportionately with body size. *Science* **360**, 642–645 (2018).
- 659 70. K. Lorenzen, The relationship between body weight and natural mortality in juvenile and
660 adult fish: a comparison of natural ecosystems and aquaculture. *Journal of Fish Biology*
661 **49**, 627–642 (1996).
- 662 71. R. B. Huey, J. G. Kingsolver, Climate warming, resource availability, and the metabolic
663 meltdown of ectotherms. *The American Naturalist* **194**, E140–E150 (2019).
- 664 72. S. Neuenfeldt, *et al.*, Feeding and growth of Atlantic cod (*Gadus morhua* L.) in the eastern
665 Baltic Sea under environmental change. *ICES Journal of Marine Science* **77**, 624–632
666 (2020).
- 667 73. J. Ohlberger, E. Edeline, L. A. Vollestad, N. C. Stenseth, D. Claessen, Temperature-driven
668 regime shifts in the dynamics of size-structured populations. *The American Naturalist* **177**,
669 211–223 (2011).
- 670 74. J. R. Brett, Energetic responses of salmon to temperature. A study of some thermal
671 relations in the physiology and freshwater ecology of sockeye salmon (*Oncorhynchus*
672 *nerka*). *Integr Comp Biol* **11**, 99–113 (1971).
- 673 75. E. E. Werner, D. J. Hall, Ontogenetic habitat shifts in bluegill: The foraging rate-predation
674 risk trade-off. *Ecology* **69**, 1352–1366 (1988).
- 675 76. E. Lloret-Lloret, *et al.*, The seasonal distribution of a highly commercial fish is related to
676 ontogenetic changes in its feeding strategy. *Front. Mar. Sci.* **7** (2020).
- 677 77. Heincke F., Rapp. Proc. Verb. Réunion. ICES 16, 1–70. (1913).
- 678 78. A. Audzijonyte, G. T. Pecl, Deep impact of fisheries. *Nature Ecology & Evolution* **2**, 1348–
679 1349 (2018).
- 680 79. H. O. Pörtner, R. Knust, Climate change affects marine fishes through the oxygen
681 limitation of thermal tolerance. *Science* **315**, 95–97 (2007).
- 682 80. W. W. L. Cheung, *et al.*, Shrinking of fishes exacerbates impacts of global ocean changes
683 on marine ecosystems. *Nature Climate Change* **3**, 254–258 (2013).
- 684 81. B. Gilbert, *et al.*, A bioenergetic framework for the temperature dependence of trophic
685 interactions. *Ecology Letters* **17**, 902–914 (2014).
- 686 82. J. A. Nelson, Oxygen consumption rate v. rate of energy utilization of fishes: a comparison
687 and brief history of the two measurements. *Journal of Fish Biology* **88**, 10–25 (2016).
- 688 83. J. D. Armstrong, L. A. Hawkins, Standard metabolic rate of pike, *Esox lucius*: variation
689 among studies and implications for energy flow modelling. *Hydrobiologia* **601**, 83–90
690 (2008).
- 691 84. A. Rohatgi, *WebPlotDigitalizer: HTML5 based online tool to extract numerical data from*
692 *plot images. Version 4.1. [WWW document] URL <https://automeris.io/WebPlotDigitizer>*
693 *(accessed on January 2019).* (2012).
- 694 85. A. Gelman, J. Hill, *Data Analysis Using Regression and Multilevel/Hierarchical Models*
695 (Cambridge University Press, 2007).
- 696 86. X. A. Harrison, *et al.*, A brief introduction to mixed effects modelling and multi-model
697 inference in ecology. *PeerJ* **6**, e4794 (2018).
- 698 87. H. Schielzeth, Simple means to improve the interpretability of regression coefficients:
699 Interpretation of regression coefficients. *Methods in Ecology and Evolution* **1**, 103–113
700 (2010).
- 701 88. F. W. H. Beamish, Respiration of fishes with special emphasis on standard oxygen
702 consumption II. Influence of weight and temperature on respiration of several species'.
703 *Canadian Journal of Zoology/Revue Canadienne de Zoologie* **42**, 177–188 (1964).
- 704 89. J. Ohlberger, G. Staaks, F. Hölker, Effects of temperature, swimming speed and body
705 mass on standard and active metabolic rate in vendace (*Coregonus albula*). *Journal of*
706 *Comparative Physiology, B* **177**, 905–916 (2007).

- 707 90. D. Padfield, M. Castledine, A. Buckling, Temperature-dependent changes to host–parasite
708 interactions alter the thermal performance of a bacterial host. *The ISME Journal* **14**, 389–
709 398 (2020).
- 710 91. R Core Team, *R: A Language and Environment for Statistical Computing*. R Foundation
711 for Statistical Computing (2020).
- 712 92. M. Plummer, JAGS: A program for analysis of Bayesian graphical models using Gibbs
713 sampling. *Working Papers*, 8 (2003).
- 714 93. M. Plummer, *rjags* (2019).
- 715 94. A. Gelman, J. Carlin, H. Stern, D. Rubin, *Bayesian Data Analysis*. 2nd edition (Chapman
716 and Hall/CRC, 2003).
- 717 95. H. Wickham, *et al.*, Welcome to the tidyverse. *Journal of Open Source Software*, 1686
718 (2019).
- 719 96. X. Fernández-i-Marín, ggmcmc: Analysis of MCMC Samples and Bayesian Inference.
720 *Journal of Statistical Software* **70**, 1–20 (2016).
- 721 97. C. Youngflesh, MCMCvis: Tools to Visualize, Manipulate, and Summarize MCMC Output.
722 *Journal of Open Source Software* **3**, 640 (2018).
- 723 98. J. Gabry, D. Simpson, A. Vehtari, M. Betancourt, A. Gelman, Visualization in Bayesian
724 workflow. *J. R. Stat. Soc. A* **182**, 389–402 (2019).
- 725 99. S. Watanabe, A Widely Applicable Bayesian Information Criterion. *Journal of Machine*
726 *Learning Research* **14**, 867–897 (2013).
- 727 100. A. Vehtari, A. Gelman, J. Gabry, Practical Bayesian model evaluation using leave-one-out
728 cross-validation and WAIC. *Stat Comput* **27**, 1413–1432 (2017).
- 729 101. M. Olmos, *et al.*, Spatial synchrony in the response of a long range migratory species
730 (*Salmo salar*) to climate change in the North Atlantic Ocean. *Global Change Biology* **26**,
731 1319–1337 (2019).
- 732 102. B. Hepher, *Nutrition of Pond Fishes* (Cambridge University Press, 1988).
- 733 103. A. D. Rijnsdorp, B. Ibelings, Sexual dimorphism in the energetics of reproduction and
734 growth of North Sea plaice, *Pleuronectes platessa* L. *Journal of Fish Biology* **35**, 401–415
735 (1989).

736

Figures and Tables

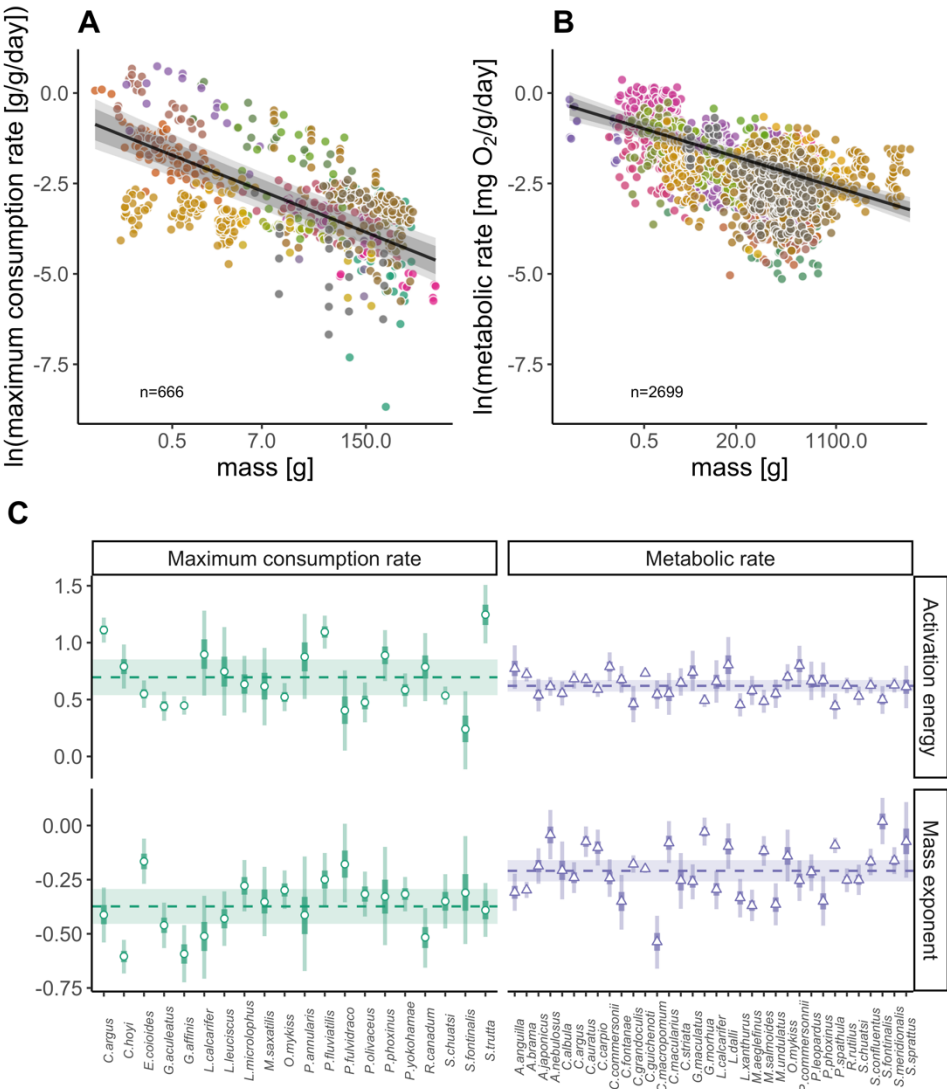


Figure 1. Natural log of mass-specific maximum consumption rate (A) and metabolic rate (B) against body mass on a logarithmic x-axis. Lines are global predictions at the average temperature in each data set (both 19°C, but note the model is fitted using mean-centred Arrhenius temperature). Shaded areas correspond to 80% and 95% credible intervals. Species are grouped by color (legend not shown, n=20 for consumption and n=34 for metabolism, respectively). C) Global and species-level effects of mass- and temperature on specific maximum consumption rate and metabolic rate. Horizontal lines show the posterior medians of the global activation energies and mass exponents of maximum consumption and metabolism (μ_{β_1} and μ_{β_2} in Eqs. 6-8 for the mass and temperature coefficients, respectively). The shaded horizontal rectangles correspond to the posterior median ± 2 standard deviations. Points and triangles show the posterior medians for each species-level coefficient (for maximum consumption rate and metabolic rate, respectively), and the vertical bars show their 80% and 95% credible interval.

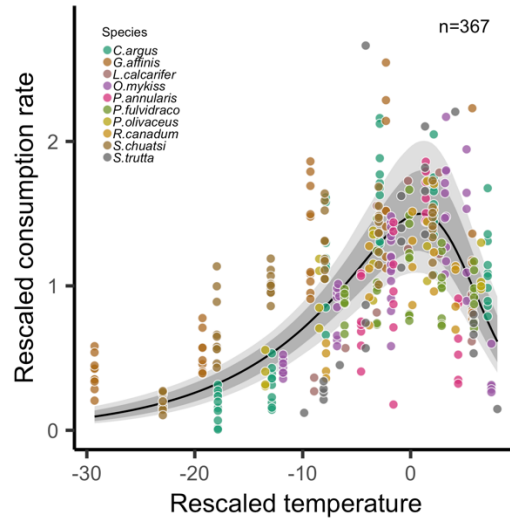


Figure 2. Mass-specific maximum consumption rate increases until a maximum is reached, after which it declines steeper than the initial rate of increase. Maximum consumption rates are relative to the average maximum consumption rates within species and temperature is the difference between the experimental temperature and the temperature where maximum consumption peaks (also by species). Lines show posterior median of predictions from the Sharpe-Schoolfield model (using the average intercept across species and the common coefficients), grey bands show 95% and 80% credible intervals. Colors indicate species.

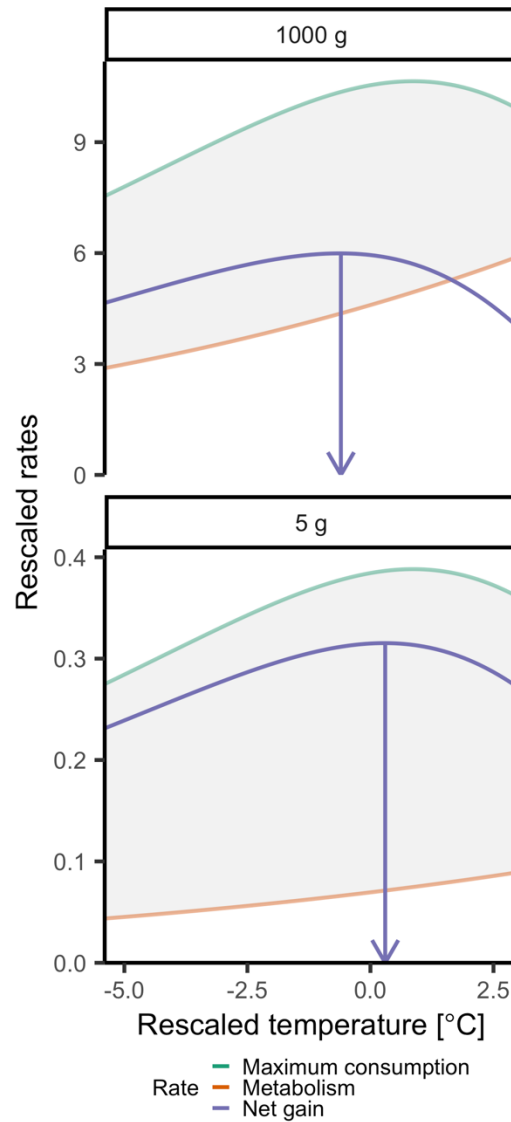


Figure 3. Illustration of predicted whole-organism maximum consumption rate (green), metabolic rate (purple) and the difference between them (orange) for two body sizes (top=1000g, bottom=5g) (see 'Materials and Methods'). Vertical arrows indicate the temperature where the difference in net energy gain (energy available for growth) is maximized for the two body sizes, which occurs at different temperatures despite that consumption peaks at the same temperature for both body sizes.

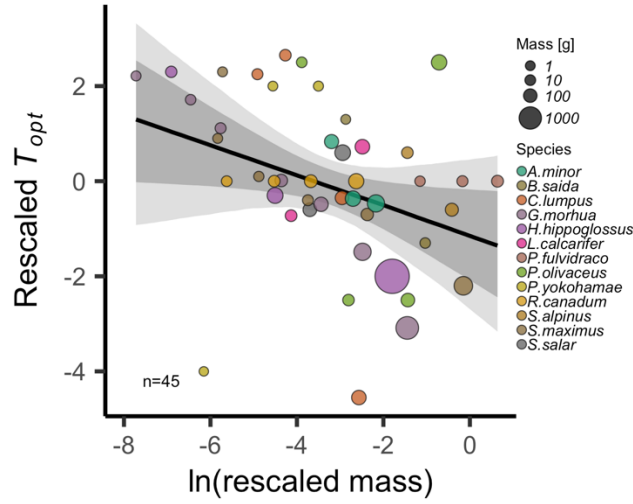


Figure 4. Experimental data demonstrating optimum growth temperature declines with body mass. The plot shows the optimum temperature within species (rescaled by subtracting the mean optimum temperature from each observation, by species) as a function of the natural log of rescaled body mass (ratio of mass to maturation mass within species). Probability bands represent 80% and 95% credible intervals, and the solid line shows the global prediction (μ_{β_0} and μ_{β_1}). Colors indicate species and the area of the circle corresponds to body mass in unit g.